## LITERATURE CITED

Benedict, M., and T. H. Pigford, *Nuclear Chemical Engineering*, McGraw-Hill, New York (1957).

Cohen, K, *The Theory of Isotope Separation as Applied to the Large-Scale Production of $U^{235}$*, McGraw-Hill, New York (1951).

Lewis, G. N., and M. Randall, *Thermodynamics and the Free Energy of Chemical Substances, McGraw-Hill, New York* (1923).

Sage, B. H., *Thermodynamics of Multicomponent Systems*, Reinhold, New York (1965).

Shachter, J., E. von Halle, and R. L. Hoglund, "Diffusion Separation Methods" in *Kirk-Othmer Encyclopedia of Chemical Technology*, Vol. 7, Interscience, New York (1965).

———, Future Structure of the Uranium Enrichment Industry, Hearings before the Joint Committee on Atomic Energy, Congress of the United States, Ninety-third Congress, First Session, on Actions Necessary to be Taken to Insure Supply of Enriched Uranium Sufficient to Meet Present and Future Needs, Part 1, Phase I: Government Witnesses (July 31 and Aug. 1, 1973).

———, *Nuclear Engineering International*, (Apr., 1977).



*Manuscript received July 18, 1977; revision received and accepted October 12, 1977.*


# A Note on Modeling Laboratory Batch Crystallizations


**T. J. McNEIL, D. R. WEED and J. ESTRIN**

**Chemical Engineering Department**
**Clarkson College of Technology**
**Potsdam, New York**


The classic analysis of Randolph and Larson (1962, 1971) serves as the basis for characterizing suspension crystallization systems. In particular, laboratory experiments employing well-mixed suspension crystallizer techniques yield crystal size distributions which are very revealing of those characteristics through application of the analysis. This has been well demonstrated with the steady state operation of the laboratory crystallizer (Randolph and Larson, 1971). The analysis of distributions from batch crystallizations is not so informative. Yet, there is a good reason for designing and carrying out experiments batchwise. For example, laboratory batch crystallizations are much more easily performed than continuous ones, especially when sampling distributions during the active crystallization period are not considered. This type of operation is particularly relevant for consideration when working with chemical systems difficult to process, for example, owing to toxic or highly viscous properties, or considerations of monetary expense; or when time to develop appropriate apparatus for continuous operation is not available; or as a first step in preparing for continuous operation in the laboratory in order to obtain experimental design information.

A particular characteristic of batch generated size distributions which appears to be encountered when the seeds charge is not too great is the plateau or hump within the domain of the distribution. This characteristic appears in the published distributions of Baliga (Randolph and Larson, 1971) and Weed (Wey and Estrin, 1973). One apparent explanation for this peculiar behavior of the distribution is size dependent growth; successful reproduction of the experimental distributions was demonstrated using this hypothesis for the potassium sulfate-water system. Other reasons for such distributions may be attrition—agglomeration phenomena and surface energy effects which may become significant at low supersaturations when the sizes influenced are within the readily measurable range.

Another reason for this behavior may be inherent in the nucleation law and typical batch operation which is associated with decreasing supersaturation as the batch proceeds. Qualitatively, the process may be described as follows: nucleation occurs initially owing to the relatively high levels of supersaturation despite low concentrations of suspended solids; in the mid period of operation, the plateau in the distribution is generated because a decrease

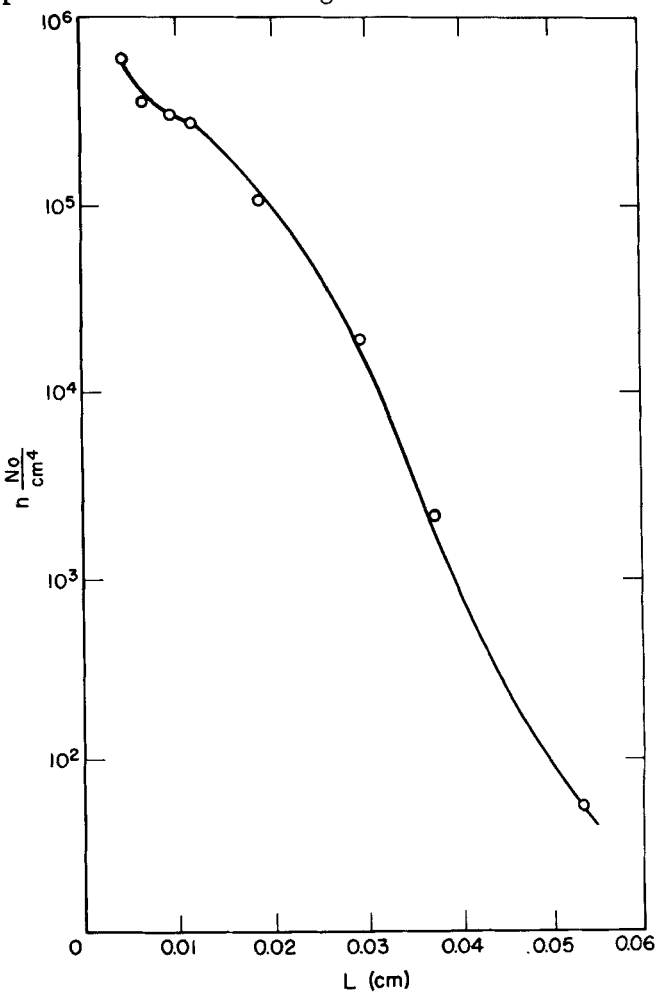


Fig. 1. Experimental size distribution: population density vs. nominal size.

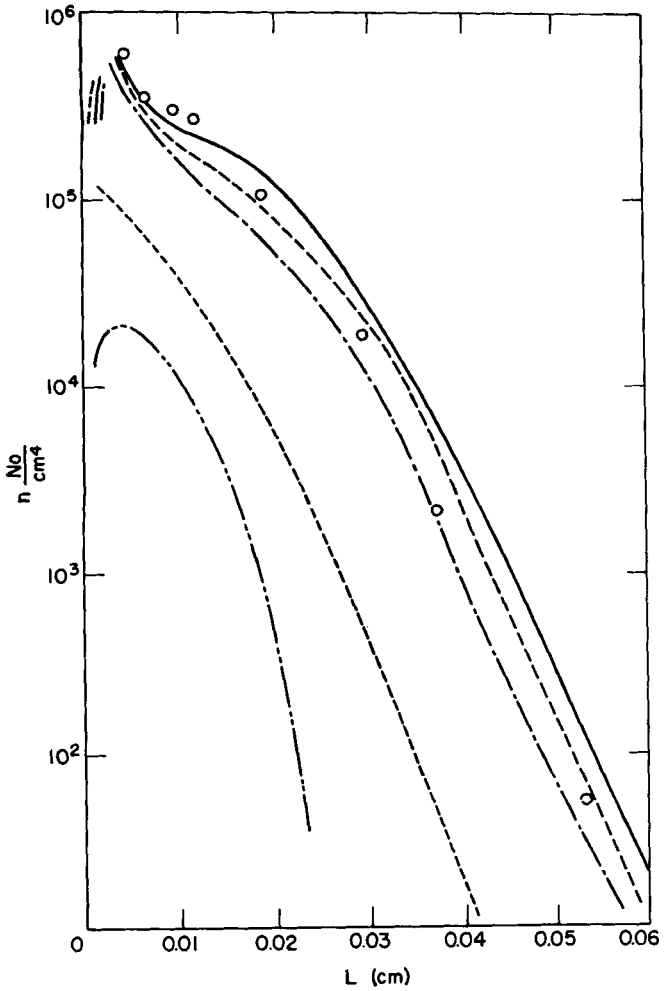


Fig. 2. Population density vs. nominal size. ○ represents experimental data as in Figure 1. Curves represent computed results, $k_1, k_2, k_3 \neq 0$; $a = 2.52 \times 10^{-3}$ cm; ——— 206 min; – – – 150 min; ——— 120 min; - - - - 60 min; ——— 30 min.

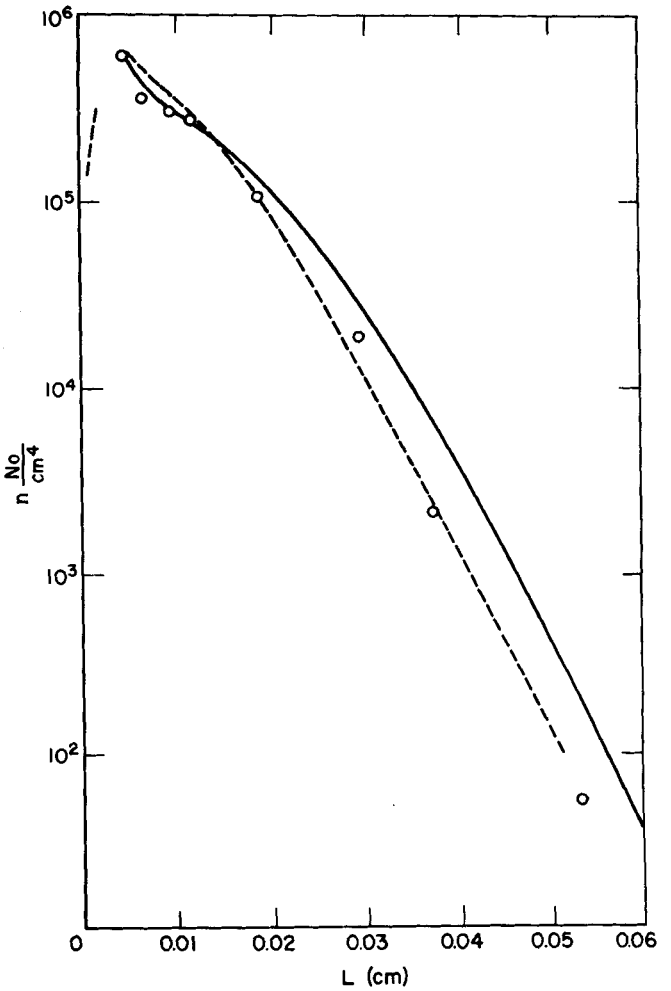


Fig. 3. Population density vs. nominal size. ○ represents experimental data as in Figure 1. Curves represent computed results: ——— $k_1, k_2, k_3, k_4, \neq 0$; $a = 3.11 \times 10^{-3}$ cm; – – – $k_1, k_2, = 0$; $a = 3.78 \times 10^{-3}$ cm.

in nucleation rate due to lower supersaturation and a less than heavy suspension. In the later period of active crystallization, even though supersaturation level has decreased, the suspension density is large enough to effect an increase in nucleation and subsequently increasing population density values. This explanation qualitatively calls upon no additional mechanisms, other than a straightforward growth model, and, say, power law nucleation behavior to influence the population-size distribution of crystals.

Recent exhaustive nucleation and growth data for the magnesium sulfate-water system have been obtained and described by Sikdar and Randolph (1976). These were obtained using the steady state, well-mixed crystallizer—Coulter counter techniques successfully employed by Randolph and co-workers in the past for other systems. Batch data for the magnesium-sulfate water system have been obtained by Weed (1972). He determined long time size distributions by sieving the contents of a Couette flow crystallizer. His major independent parameter was the rotational velocity of the inner wall of the crystallizer, but this is not of relevance here except to note that a dependence of nucleation upon revolutions per minute was observed but was far from conclusive. However, Weed's distributions did exhibit the characteristic hump. Of significance is that the nucleation and growth rate results of Sikdar and Randolph were revolutions per minute independent. Furthermore, the growth rate was size independent over the range 15 to 70 $\mu$ and probably greater, and the nucleation rate was dependent upon suspension density. The expressions obtained by Sikdar and Randolph for the magnesium sulfate system, for growth, $G$, and nucleation $B^o$ rates are reproduced here:

$$G = \exp(4.895)\, s^{2.29} \quad (1)$$

$$B^o = \exp(-56.05)\, s^{2.59} \exp(21\,346/T)\, M_T^{0.67} \quad (2)$$

Weed's data are shown graphically in Figure 1. The availability of both these sets of data provides an opportunity to evaluate the hypothesis noted earlier concerning the reason for the plateau in the batch-generated distribution.

Weed's apparatus and experimental procedure are described elsewhere (1972). Briefly, the apparatus consisted of a crystallizing volume located in an annulus between stainless cylinders 7.62 and 9.55 cm in diameter; the length of the outer wall was 33.0 cm. The effective volume of the suspension reported upon here was 0.928 l. Both rotor and stator surfaces exposed to the active volume were cooled by circulating coolant. The rotor velocity for the run reported upon here was 1 000 rev/min. This run was typical of a total of four made at the same conditions. These crystallizations were isothermal (33.9°C) in the sense that the coolant temperature was held constant, and the initial supersaturation was 1.1°C for all. The supersaturated solution was seeded with one well-formed crystal whose short dimension was 0.0865 cm. The run described here was typical of four made at the same conditions, for which observed agglomeration effects were minimal. Population density-size data are shown in Figure 1 for a typical run.

The batch process described above was mathematically modeled using the moments procedure described by Hulburt and Katz (1964). The problem solved is given partially by the population balance as follows:

$$\frac{\partial n}{\partial t}(t, L) + G[s(t)]\frac{\partial n}{\partial t}(t, L) = 0 \qquad (3)$$

$$\mu_o(0) \equiv \int_o^\infty n(0, L)dL = 100 \qquad (4a)$$

$$\mu_i(0) \equiv \int_o^\infty L^i n(0, L)dL = 0, \quad i = 1, 2, \ldots \qquad (4b)$$

$$\frac{d\mu_o}{dt}(t) = B^o[s(t), M_T(t), T_B(t)] \qquad (5)$$

The functions $G[s(t)]$ and $B^o[S(t), M_T(t), T_B(t)]$ are given by Equations (1) and (2) and

$$M_T(t) = \mu_3(t)\rho_c \cdot k_v \qquad (6)$$

The material balance may be formed to give the bulk concentration of solute

$$C_B = \frac{K_w - \rho_c k_v \mu_3}{1 - k_v \mu_3} \qquad (7)$$

and the energy balance, to sufficient accuracy, may be expressed as

$$\frac{dT_B}{dt} = \{3\rho_s\lambda G\mu_2 + UA_v(T_c - T_B) + U_L A_L(T_{SR} - T_B) + P_v\}/\{(1 - k_v\mu_3) \times (\rho_s - C_B)c_{PW} + (1 - k_v\mu_3)C_B c_{PC} + k_v\mu_3\rho_c c_{PC}\} \qquad (8)$$

The initial conditions required for $C_B$ and $T_B$ are known experimental values corresponding to the initial supersaturation.

Aside from an estimate of $\mu_o(0)$, discussed further below, and several operating condition parameters, no adjustable constants are involved. Ordinary differential equations for successive moments were generated from Equation (3) together with the initial and boundary conditions (4) and (5) and the material and energy balances; these were solved by fourth-order Runge-Kutta integration. The moments resulting permitted recovery of the distribution as described in Hulburt and Katz (1964) and discussed in Randolph and Larson (1971). The value for $\mu_o(0)$ above was an arbitrary value; Weed had shown in his preliminary modeling (1972) that the final distributions were not sensitive to $\mu_o(0)$. Although experimentally one seed of finite size was introduced, this was considered only as providing initially bred secondary nuclei of size, $L \to 0$, so that $\mu_o(0)$ was the only nonzero moment at zero time.

For recovery of the moments, the distribution was expressed as an expansion in orthogonal polynomials about the weighting function $\exp(-L/a)$. The population density functions becomes

$$n(t, L) = \frac{1}{a}\exp\left(-\frac{L}{a}\right)\left[\mu_o + \sum_{n=1}^{l} k_n L_n\left(\frac{L}{a}\right)\right] \qquad (9)$$

where $l$ represents the moment of highest order considered, where $a$ was determined by extrapolating the data displayed in Figure 1 to $L = 0$, and

$$a = \frac{\mu_o(\text{experimental})}{n(t, 0)\,(\text{from extrapolation})}$$

In this way, we considered the weighting function to be forced to roughly estimate the experimental distribution but showing no structural details (particularly the plateau). Actually, we also applied the Laguerre series as described by Hulburt and Katz, in which $k_1$ and $k_2$ are made to equal zero by appropriate choices of $a$ and the second parameter in the $\Gamma$-distribution weighting function. The resulting distributions were equivalent to those given here. The $k_n$ are functions of the moments derived from the solutions in time of the differential equations; for example, $k_o = \mu_o$.

The results are shown in Figure 2 as population density vs. size. The expansion included the $k_3 L_3$ term. The solid curve shown represents Weed's data as shown in Figure 1. The location of the plateau did not change with different choices for $a$, although the qualitative appearance did somewhat. Figure 3 shows the distributions obtained when different $a$ values and truncation choices were employed. However, the use of higher moments did result in distributions which were not as good as those exhibited here.

It appears evident from Figures 2 and 3 that the plateau in the population density-size distribution may well be due to the competition between growth and nucleation for dissolved solute. It is not necessary to call upon other mechanisms or complicated growth functions to explain this characteristic of the distribution. If one considers that this is an acceptable explanation, then a modeling procedure devised to simulate this characteristic can be useful in revealing nucleation and growth expression parameter values from batch crystallization experiments.


## ACKNOWLEDGMENT

The authors acknowledge that this work was supported in part by the NSF through grant ENG 75-04988.


## NOTATION

$a$ = parameter in expansion for $n(t, L)$, $(\text{cm})^{-1}$
$A_v$ = heat transfer area, system to coolant, per unit active volume $(\text{cm})^{-1}$
$A_L$ = heat transfer area for heat loss to surroundings per unit active volume, $(\text{cm})^{-1}$
$B^o$ = nucleation rate, (No.) $(\text{cm}^3)^{-1}$ $(\text{s}^{-1})$
$C_B$ = volume concentration of solute, (g) $(\text{cm}^3)^{-1}$
$c_{PC}$ = heat capacity of solids, (J) $(\text{g})^{-1}$ $(°\text{C})^{-1}$
$c_{PW}$ = heat capacity of water, (J) $(\text{g})^{-1}$ $(°\text{C})^{-1}$
$G$ = growth rate, (cm) $(\text{s})^{-1}$
$k_v$ = volumetric shape factor, dimensionless
$k_n$ = expansion coefficient in Equation (9)
$K_W$ = total mass of solute charge to crystallizer per unit volume, (g) $(\text{cm}^3)^{-1}$
$L$ = characteristic size of crystal, (cm)
$M_T$ = suspended solids concentration, (g) $(\text{cm}^3)^{-1}$
$n$ = population density, (No.) $(\text{cm}^3)^{-1}$ $(\text{cm})^{-1}$
$P_v$ = power dissipated by agitation per unit volume, (J) $(\text{s})^{-1}$ $(\text{cm}^3)$
$s$ = supersaturation, (g anhydrous solute) (g water)$^{-1}$
$t$ = time
$T$ = absolute temperature (°K)
$T_B$ = suspension temperature (°C)
$T_c$ = coolant temperature (°C)
$T_{SR}$ = surroundings temperature (°C)
$U$ = heat transfer coefficient for heat transfer surface of active volume, (J) $(\text{s})^{-1}$ $(\text{cm}^2)^{-1}$ $(°\text{C})^{-1}$
$U_L$ = heat transfer coefficient for heat transfer surface to surroundings, (J) $(\text{s})^{-1}$ $(\text{cm}^2)^{-1}$ $(°\text{C})^{-1}$
$\rho_c$ = density of solids, (g) $(\text{cm}^3)^{-1}$
$\rho_s$ = density of solution, (g) $(\text{cm}^3)^{-1}$
$\lambda$ = heat of solution, (J) $(\text{g})^{-1}$
$\mu_i$ = $i^{\text{th}}$ moment, $\mu_i \equiv \int_o^\infty L^i dL$

## LITERATURE CITED

Hulburt, H. M., and S. Katz, "Some Problems in Particle Technology. A Statistical Mechanical Formulation," *Chem. Eng. Sci.*, **19**, 555 (1964).

Randolph, A. D., and M. A. Larson, *Theory of Particulate Processes*, Academic Press, New York (1971).

———, "Transient and Steady State Size Distributions in Continuous Mixed Suspension Crystallizers," *AIChE J.*, **8**, 639 (1962).

Sikdar, S. K., and A. D. Randolph, "Secondary Nucleation of Two Fast Growth Systems in a Mixed Suspension Crystallizer: Magnesium Sulfate and Citric Acid Water Systems," *ibid.*, **22**, 110 (1976).

Weed, D. R., "Growth and Nucleation Studies for a Batch, Isothermal, Suspension Crystallizer" M.S. thesis, Clarkson College of Technology, Potsdam, N.Y. (1972).

Wey, J-S, and J. Estrin, "Modeling the Batch Crystallization Process. The Ice-Brine System," *Ind. Eng. Chem. Process Design Develop.*, **12**, 236 (1973).



*Manuscript received January 20, 1977; revision received October 14, and accepted October 27, 1977.*


# Vapor Pressures of High-Boiling Liquid Hydrocarbons


**A. B. MACKNICK**
**JACK WINNICK**
**and**
**J. M. PRAUSNITZ**

**Chemical Engineering Department**
**University of California,**
**Berkeley, California**


Owing to the rising importance of coal-derived fluids and heavy petroleum in emerging technology, the vapor pressures of heavy hydrocarbons are becoming of increasing interest in chemical process design. In this note we consider how limited liquid vapor-pressure data, obtained at near-ambient temperatures, can be used to predict vapor pressures at elevated temperatures where industrial processes often occur but where it is difficult to make experimental measurements.

We consider four methods for extrapolating vapor pressures $P$ to higher temperatures $T$:

1. The linear method, wherein a plot of log $P$ vs. $T^{-1}$ is assumed to be a straight line.
2. The method of Riedel (1954) which requires critical temperature, critical pressure, and one vapor-pressure datum.
3. The method of Zia and Thodos (1974) which also requires critical temperature, critical pressure, and one vapor-pressure datum.
4. The SWAP method (Smith et al., 1976) which requires only approximate information on the molecular structure of the hydrocarbon and one vapor-pressure datum.

Critical temperatures and pressures can be estimated using the method of Foreman and Thodos as described in Reid and Sherwood (1966), provided the molecular structure of the hydrocarbon is known. Particularly important is the number of carbon atoms per molecule.

Detailed consideration was not given to the Antoine equation because a preliminary study showed that when the Antoine parameters were determined from limited vapor-pressure data, the resulting equation, while good for interpolation, is extremely poor for extrapolation.

For our study we used five representative hydrocarbon liquids that have been studied experimentally. They are eicosane (I), 1,1 dicyclohexyl heptane (II), 2,2,4,10,12,12 hexamethyl-7-(3,5,5,-trimethylhexyl)-6-tridecane (III), perhydrochrysene (IV) and 9-N-butylanthracene (V).

Table 1 gives the measured temperature corresponding to a vapor pressure of 0.01 Torr. This temperature, always above the melting point, is the experimental datum used in all four extrapolation methods.

Table 1 also gives estimated critical temperatures and pressures and, where appropriate, the fraction of carbon atoms which are aromatic ($F_A$), naphthenic ($F_N$), or branched ($F_B$). These fractions are required in the SWAP method.

Calculated and experimental vapor pressures are compared in Table 1 which gives the percent error at two temperatures: $T_1$ and $T_{10}$ where the subscript refers to the observed pressure in torr. All experimental data are from American Petroleum Institute Projects 42 and 44, except $T_{0.01}$ for eicosane which was measured in our own laboratory.

The simplest manner for using the linear method, log $P$ vs. $T^{-1}$, is to interpolate between $T_{0.01}$ and the estimated critical point. However, this procedure calculates pressures in error by an order of magnitude. Instead, several experimental data in the region 0.001 to 0.01 torr were fit to a straight line. The equation of this line was then used to estimate $T_1$ and $T_{10}$.

Calculations using the method of Riedel are described by Reid et al. (1977). Calculations using the method of Zia and Thodos are described by those authors (Zia and Thodos. 1974).

Calculations using the SWAP method are essentially those described by Smith et al. (1976) but require, in addition, an empirical relation between $T_{760}$ and $T_{0.01}$ for normal paraffins. From available experimental data, this relation is

$$T_{760} = 3.22 + 2.089\,T_{0.01} - 1.035 \times 10^{-3}(T_{0.01})^2 \qquad (1)$$

Equation (1) above replaces Equation (13) in the article by Smith et al. (1976).

The results in Table 1 indicate that the linear method is poor; the other three methods are consistently better, but it appears that of these three, no one method is significantly better than the others. However, the method of Riedel and that of Zia and Thodos require detailed information on molecular structure, in particular, the number of carbon atoms per molecule; this information is


Jack Winnick is at the University of Missouri, Columbia, Missouri 65201.